Supporting Information

Mullins et al. 10.1073/pnas.0906781106

SI Text

Detection of Calcium Binding by $^{45}Ca^{2+}$ Overlay. The $^{45}CaCl_2$ (1 mCi, 37 MBq) was obtained from NEN. The general method of $^{45}Ca^{2+}$ overlay has been described in detail elsewhere (1). Our specific conditions were as follows: Purified GST-fusion peptides (2 and 10 μg per lane) and CaM (0.5 μg per lane) were transferred to a PVDF membrane after 13% SDS PAGE. The blot was extensively washed for 3 $\times$ 10 min with binding buffer (60 mM KCl, 5 mM $MgCl_2$, and 10 mM imidazole-HCl, pH 6.8) to remove electrode buffer. The overlay assay was performed by incubating the blot with 8.8 μM $^{45}CaCl_2$ (10 mCi/mg; NEN) in 20 mL of binding buffer at 25 °C for 1 h, followed by 3 $\times$ 2-min washes in dH_2O and a 2 min wash in 50% ethanol. After air drying, the blot was exposed to Hyperfilm (GE Healthcare). After autoradiography the blot was stained in 40% methanol, 10% acetic acid, and 0.1% Coomassie brillant blue R250, and destained in 20% methanol and 7% acetic acid.

Primers Used in Generating Constructs. ***Cherry-STIM1$_{1-448}$.*** Forward, CTGGCATCCACTAACTGGTGGCTGC; reverse, gCAGCCACCAGTTAGTGGATGCCAG.
GFP-STIM1$_{1-469}$. Forward, CGCCCCAACCCTGCTTAGTTCATCATGACTGAC; reverse, GTCAGTCATGATGAACTAAGCAGGGTTGGGGCG.
GFP-STIM1$_{1-491}$. Forward, CCCTTGTCCATGCAGTGACCTAGCCTGCAGAGC; reverse GCTCTGCAGGCTAGGTCACTGCATGGACAAGGG.
GFP-STIM1$_{1-513}$. Forward, CATGGCCTGGGATCTCAGTAGGATTTGACCCATTCC; reverse, GGAATGGGTCAAATCCTACTGAGATCCCAGGCCATG.
GFP-STIM1$_{1-560}$. Forward, GGCAGCCACCGGCTGATCTAGGGGGTCCACCCAGGG; reverse, CCCTGGGTGGACCCCCTAGATCAGCCGGTGGCTGCC.
GFP-STIM1$_{1-630}$. Forward, GACACACCATCTCCAGTTTAGGACAGCCGAGCCCTG; reverse, CAGGGCTCGGCTGTCCTAAACTGGAGATGGTGTGTC.
Cherry-STIM1$_{1-672}$. Forward, GACTCCAGCCCAGGCTGAAAGAAGTTTCCTCTC; reverse, GAGAGGAAACTTCTTTCAGCCTGGGCTGGAGTC.
YFP-STIM1$_{234-448}$. Forward, AACCGTTACTCCAAGGAGCAC; reverse, GAATTCAGTGGATGCCAGGGTTGTTG.
YFP-STIM1$_{342-469}$. Forward, GGATCCATGTATGCTCCAGAGGCCCTTC; reverse, TCAAGCAGGGTTGGGGCGTGTACTGCC.
YFP-STIM1$_{342-560}$. Forward, GGATCCATGTATGCTCCAGAGGCCCTTC; reverse, TCAGATCAGCCGGTGGCTGCCATTGGAAGT.
YFP-STIM1$_{342-630}$. Forward, GGATCCATGTATGCTCCAGAGGCCCTTC; reverse, TCAAACTGGAGATGGTGTGTCTGG.
myc-STIM1 478,481 DD → GG. Forward, ATGACTGACGACGTGGGTGACATGGGTGAGGAGATTGTGTCTCCC; reverse, GGGAGACACAATCTCCTCACCCATGTCACCCACGTCGTCAGTCAT.
myc-STIM1 4A2G (from myc-STIM1 478,481 DD → GG). Forward, CACTTCATCATGACTGCCGCCGTGGGTGACATGGGTGCGGCGATTGTGTCTCCC; reverse, GGGAGACACAATCGCCGCACCCATGTCACCCACGGCGGCAGTCATGATGAAGTG.
GFP-STIM1 475/476 DD → AA. Forward, CACTTCATCATGACTGCAGcCGTGGATGACATGGAT; reverse, ATCCATGTCATCCACGGCTGCAGTCATGATGAAGTG.
GFP-STIM1 482,483 EE → AA. Forward, GACGTGGATGACATGGATGCGGCGATTGTGTCTCCCTTG; reverse, CAAGGGAGACACAATCGCCGCATCCATGTCATCCACGTC.
Orai1$_{1-91}$ (in myc-Orai1 and GFP-myc-Orai1). Forward, CTTAAAGCCTCCAGCCGGTGATCGGCTCTGCTCTCC; reverse, GGAGAGCAGAGCCGATCACCGGCTGGAGGCTTTAAG.
Orai1 A73E (in myc-Orai1 and GFP-myc-Orai1$_{1-91}$). Forward, GAGCACTCCATGCAGGAGCTGTCCTGGCGCAAG; reverse, CTTGCGCCAGGACAGCTCCTGCATGGAGTGCTC.
Orai1 W76E (in myc-Orai1 and GFP-myc-Orai1$_{1-91}$). Forward, ATGCAGGCGCTGTCCGAGCGCAAGCTCTACTTG; reverse, CAAGTAGAGCTTGCGCTCGGACAGCGCCTGCAT.
Orai1 Y80E (in myc-Orai1 and GFP-myc-Orai1$_{1-91}$). Forward, TCCTGGCGCAAGCTCGAGTTGAGCCGCGCCAAG; reverse, CTTGGCGCGGCTCAACTCGAGCTTGCGCCAGGA.
Orai1 W76A (in myc-Orai1 and GFP-myc-Orai1$_{1-91}$). Forward, ATGCAGGCGCTGTCCGCGCGCAAGCTCTACTTG; reverse CAAGTAGAGCTTGCGCGCGGACAGCGCCTGCAT.
Orai1 W76S (in myc-Orai1 and GFP-myc-Orai1$_{1-91}$). Forward, ATGCAGGCGCTGTCCAGTCGCAAGCTCTACTTG; reverse, CAAGTAGAGCTTGCGACTGGACAGCGCCTGCAT.
Orai1 Y80A (in myc-Orai1 and GFP-myc-Orai1$_{1-91}$). Forward, TCCTGGCGCAAGCTCGCGTTGAGCCGCGCCAAG; reverse, CTTGGCGCGGCTCAACGCGAGCTTGCGCCAGGA.
Orai1 Y80S (in myc-Orai1 and GFP-myc-Orai1$_{1-91}$). Forward, TCCTGGCGCAAGCTCAGTTTGAGCCGCGCCAAG; reverse, CTTGGCGCGGCTCAAACTGAGCTTGCGCCAGGA.
Calmodulin (CaM). Forward, GCCACCATGGCTGATCAGCTGACTGAAGAACAG; reverse, GGATCCTCATTTTGCAGTCATCATCTGTAC.
CaM-T27C. Forward, AAGGATGGAGATGGCTGTATCACCACCAAGGAG; reverse, CTCCTTGGTGGTGATACAGCCATCTCCATCCTT.
STIM1$_{470-491}$. Forward, GGATCCATGCACTTCATCATGACTGACGACGTG; reverse, TCACTGCATGGACAAGGGAGACAC.

1. Maruyama K, Mikawa T, Ebashi S (1984) Detection of calcium binding proteins by ^{45}Ca autoradiography on nitrocellulose membrane after sodium dodecyl sulfate gel electrophoresis. *J Biochem* 95:511–519.

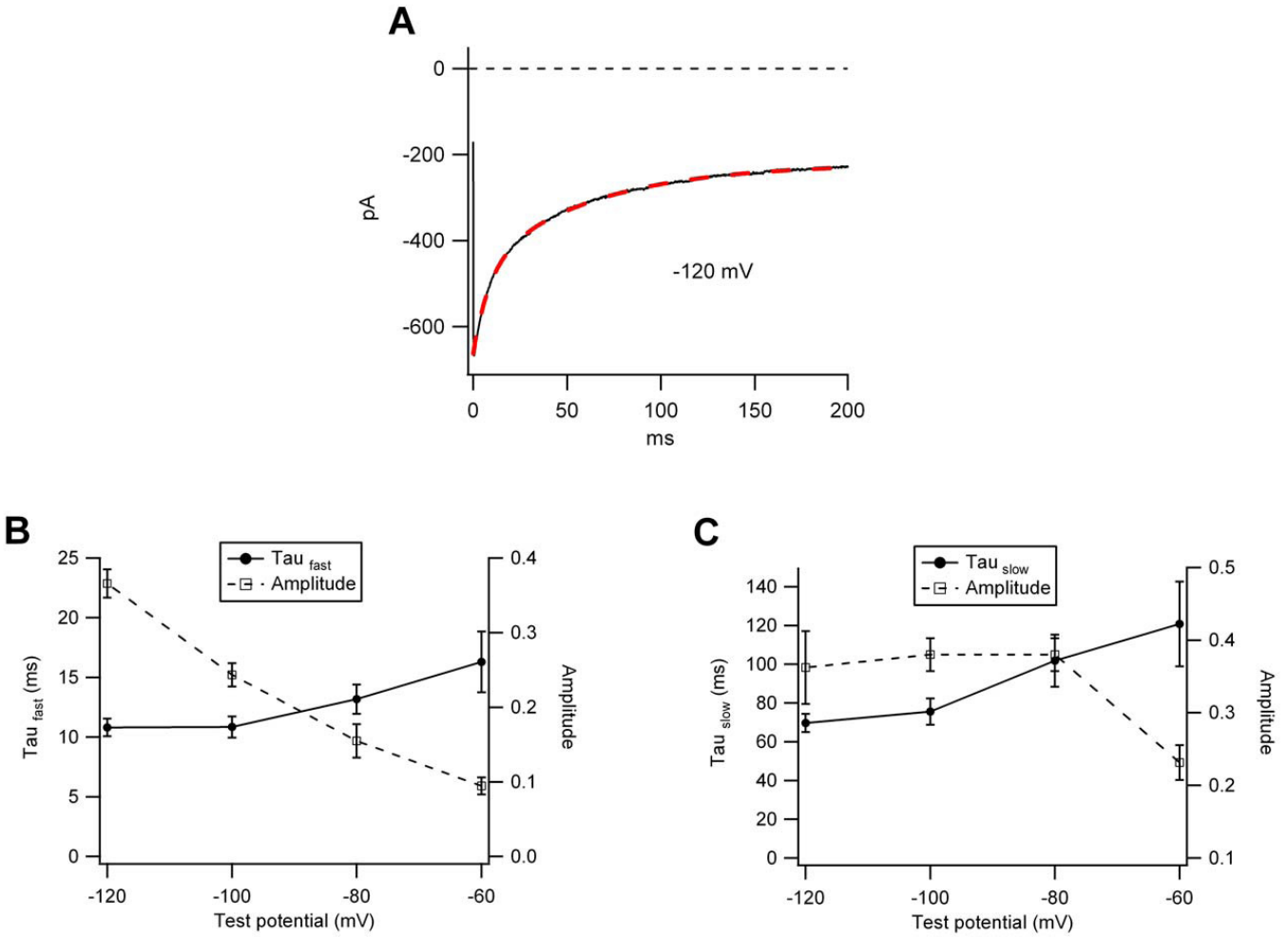

Fig. S1. Inactivation kinetics of heterologously expressed Ca^{2+} release-activated Ca^{2+} (CRAC) channels. Currents were elicited in 20 mM $Ca^{2+}{}_o$ in HEK293 cells cotransfected with myc-Orai1 + GFP-STIM1 as described in Fig. 1*A*, and fitted by the relation $I = I_o + A_1 e^{-t/\tau 1} + A_2\, e^{-t/\tau 2}$ (see *Materials and Methods*). (*A*) Representative fit (red dashed line) to current elicited by a step to −120 mV (black). (*B*) Fast time constants and amplitudes of inactivation plotted against test potential. Each point shows the mean ± SEM of five cells. (*C*) Slow time constants and amplitudes of inactivation plotted against test potential. Each point shows the mean ± SEM of five cells.

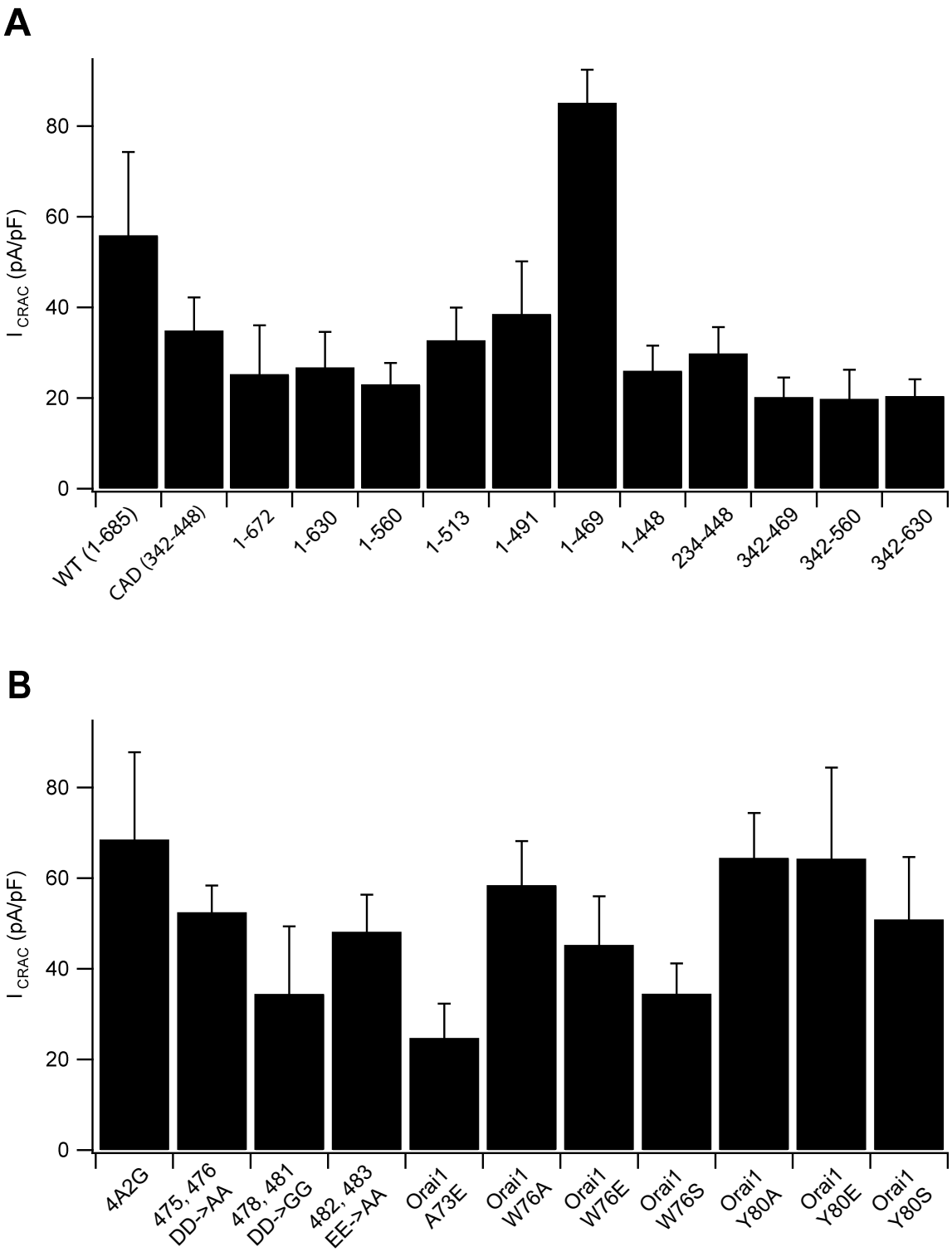

Fig. S2. Comparison of current densities for STIM1 and Orai1 constructs. HEK293 cells were cotransfected with myc-Orai1 and the indicated STIM1-derived constructs, or GFP-STIM1 and the indicated Orai1-derived constructs, and I_{CRAC} was allowed to reach a maximal level of induction. For each cell, peak current was measured 3 ms after stepping to −100 mV in 20 mM $Ca^{2+}{}_o$ and normalized to the cell capacitance. Each bar shows the mean ± SEM of 5–10 cells for each construct. Although significant cell–cell variability was seen (as expected for transient transfection experiments), average current densities were similar for most constructs tested.

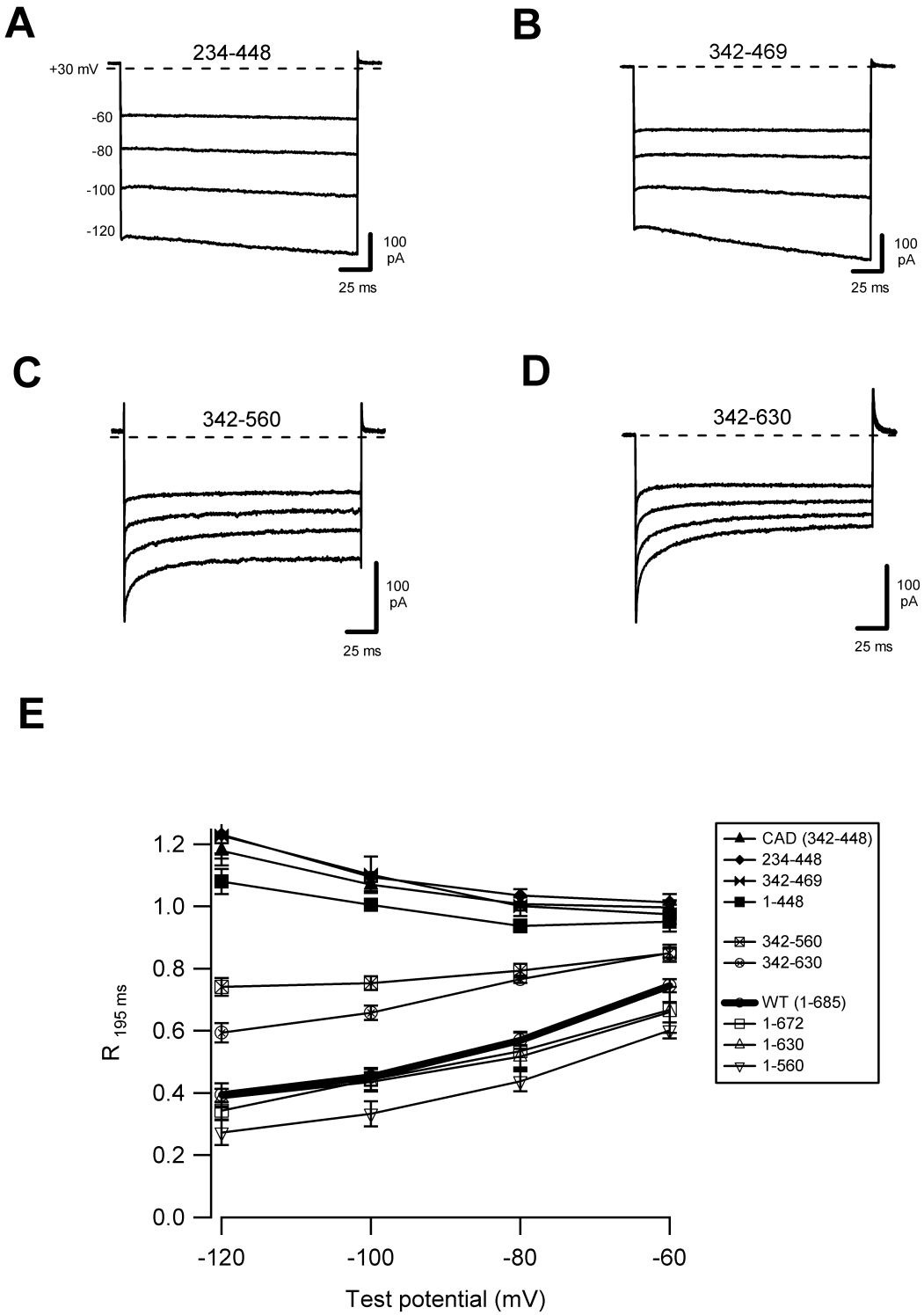

Fig. S3. Effects of extending the CRAC activation domain (CAD) peptide on Ca^{2+}-dependent inactivation (CDI). Currents were elicited in 20 mM Ca^{2+}_o in HEK293 cells cotransfected with myc-Orai1 and the indicated CAD-derived construct. All currents were constitutively active, with large currents present at the first pulse after break-in. (*A–D*) Representative currents during pulses to the indicated voltages for YFP-STIM1$_{234-448}$ (*A*), YFP-STIM1$_{342-469}$ (*B*), YFP-STIM1$_{342-560}$ (*C*), and YFP-STIM1$_{342-630}$ (*D*). (*E*) Extent of inactivation, quantified as the residual current remaining at the end of the test pulse ($R_{195\ ms} = I_{195\ ms}/I_{3\ ms}$), plotted against test potential. Each point represents the mean ± SEM of five to six cells. Data from Fig. 1*E* are included in the summary graph for comparison purposes. Extending CAD to amino acids 560 or 630 only partially rescues inactivation relative to STIM1$_{1-560}$ or STIM1$_{1-630}$.

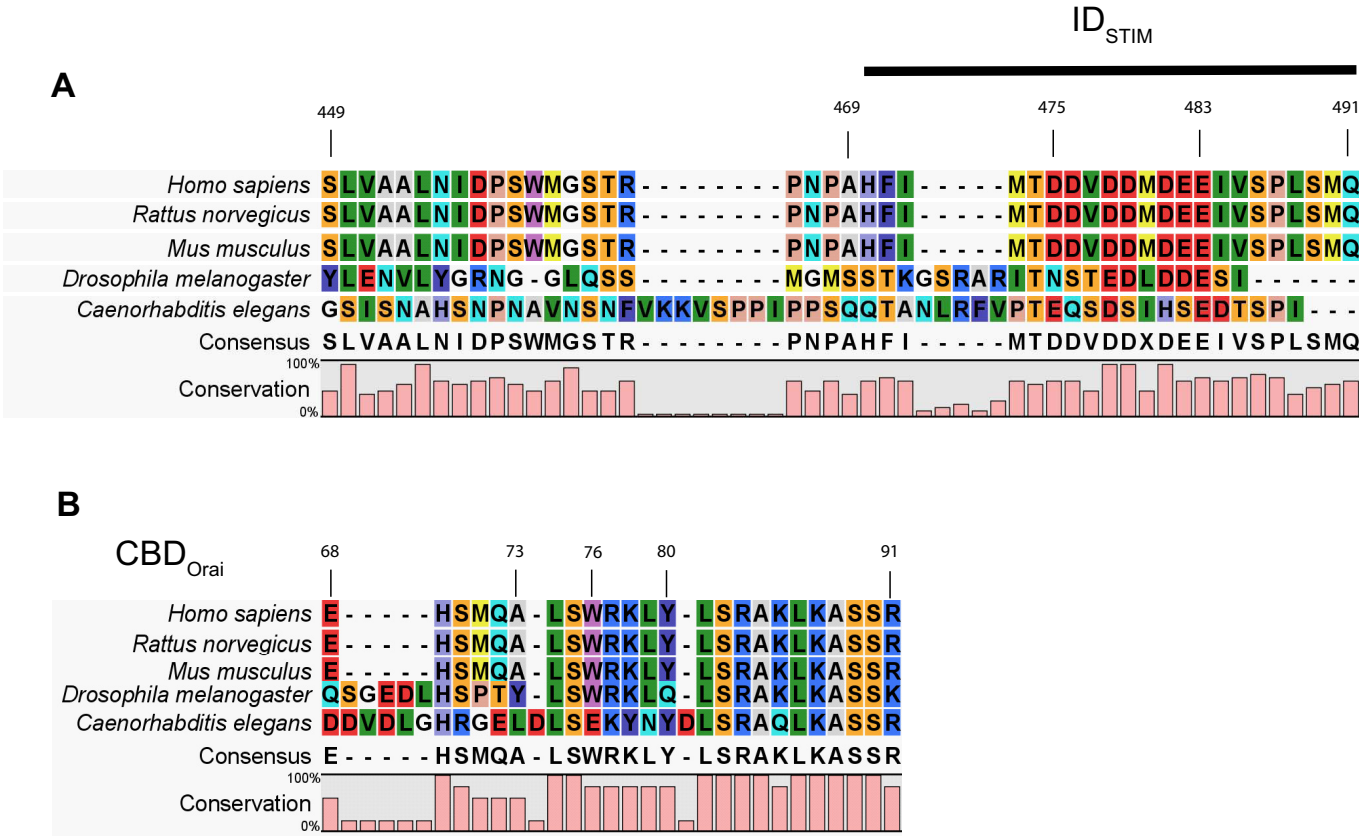

Fig. S4. Alignment of ID_{STIM} and CBD_{Orai} sequences. (*A*) Full-length STIM1 amino acid sequences from vertebrate and invertebrate species were aligned with CLC Sequence Viewer version 5 using default settings. The region corresponding to amino acids 449–491 of human STIM1 is shown, and the ID_{STIM} (amino acids 470–491) is annotated (bar). The degree of conservation for each position is shown at the bottom. Although a high degree of sequence conservation is seen in this region among vertebrates, greater variability is seen among invertebrates, leading to the introduction of several gaps. (*B*) Full-length Orai1 amino acid sequences from vertebrate and invertebrate species were aligned with CLC Sequence Viewer version 5 using default settings. The region corresponding to amino acids 68–91 of human Orai1 is shown. The degree of conservation for each position is shown at the bottom. The residues A73, W76, and Y80, all key for inactivation (Fig. 4), are highly conserved in vertebrates, but variable among invertebrates.

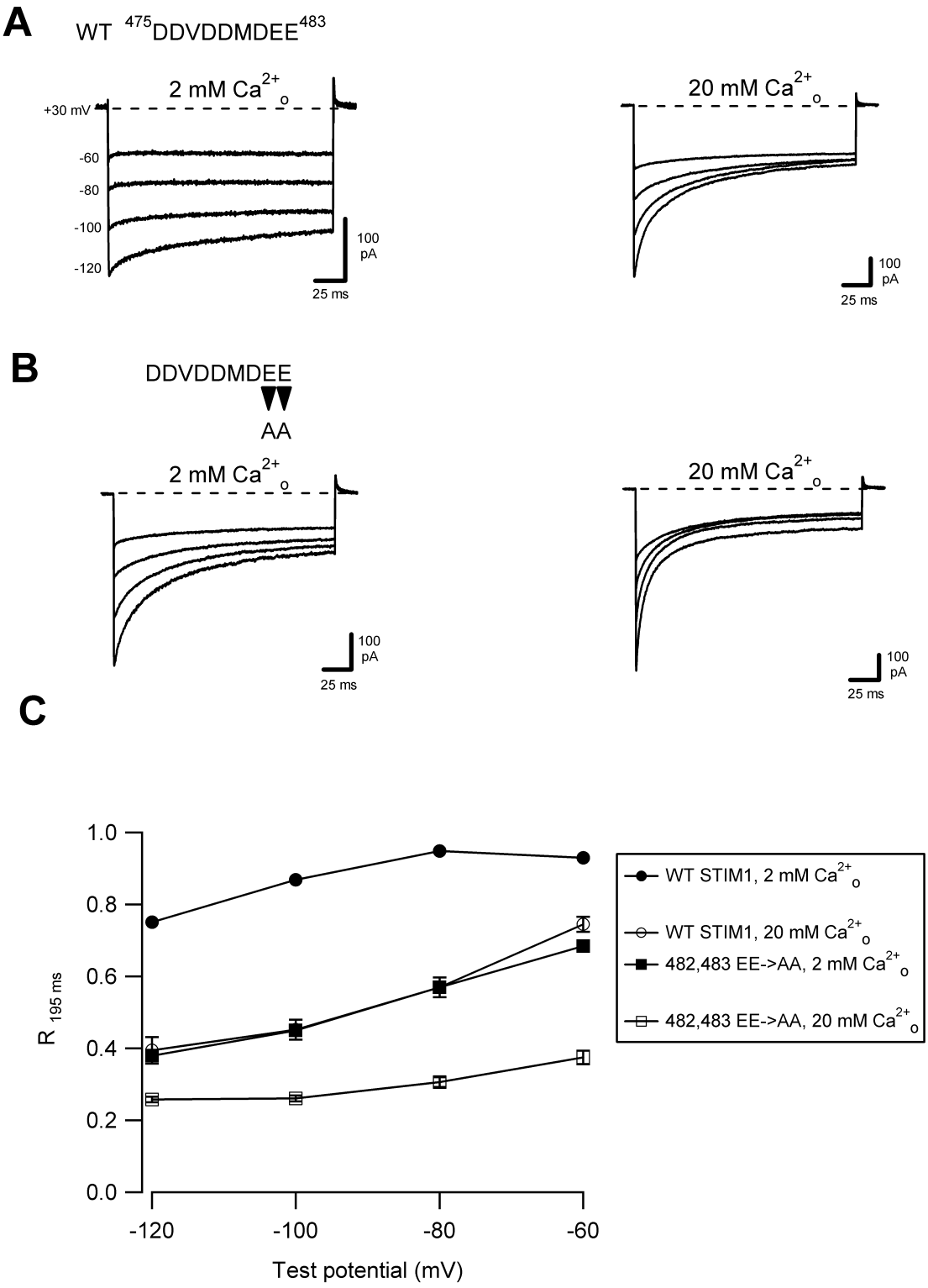

Fig. S5. The 482/483 EE → AA mutation in STIM1 increases the calcium sensitivity of I_{CRAC} inactivation. Currents were recorded in HEK293 cells cotransfected with myc-Orai1 and the indicated STIM1-derived construct, after induction of I_{CRAC} reached a maximum. (*A*) Representative currents evoked by WT GFP-STIM1 recorded in 2 (*Left*) or 20 (*Right*) mM $Ca^{2+}{}_o$ during pulses to the indicated voltages. Traces in 20 mM $Ca^{2+}{}_o$ are reproduced from Fig. 1*A*. (*B*) Representative currents evoked by STIM1 482/483 EE → AA recorded in 2 (*Left*) or 20 (*Right*) mM $Ca^{2+}{}_o$. Note the presence of strong inactivation even in low $[Ca^{2+}]_o$, unlike the WT traces in *A*. Traces in 20 mM $Ca^{2+}{}_o$ are reproduced from Fig. 2*E*. (*C*) Extent of inactivation for WT and 482/483 EE → AA plotted against test potential. Each point represents the mean ± SEM of five cells (WT, 20 mM $Ca^{2+}{}_o$) or 7 cells (482/483 EE → AA, 20 mM $Ca^{2+}{}_o$). For 2 mM $Ca^{2+}{}_o$, $n = 1$ cell for both constructs.

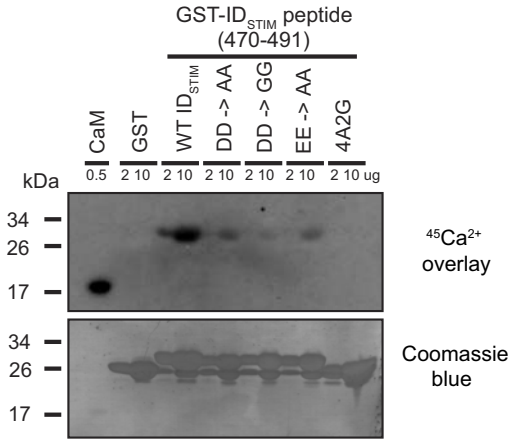

Fig. S6. Ca^{2+} binding to the ID_{STIM} domain detected by $^{45}Ca^{2+}$ overlay. Purified CaM (0.5 μg) and GST (2 and 10 μg) were loaded for controls. WT and mutant GST-STIM1 peptides corresponding to amino acids 470–491 were tested. (*Upper*) CaM, WT GST-ID_{STIM} 470–491, and GST-fused peptides in which 2 aa were mutated were able to bind to Ca^{2+} to variable degrees. No Ca^{2+} binding was detected for GST or the 4A2G mutant. (*Lower*) Coomassie staining shows loaded proteins.

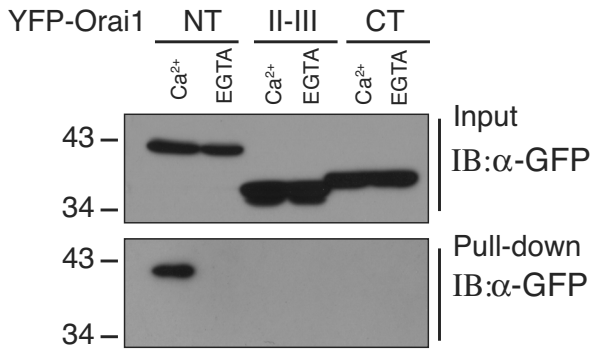

Fig. S7. CaM Sepharose pull-down confirming Ca^{2+}-dependent binding of CaM to the Orai1 N terminus. Lysates from HEK 293T cells expressing YFP-tagged N-terminal, II-III loop, and C-terminal fragments of Orai1 were applied to CaM-Sepharose in the presence of 2 mM Ca^{2+} or 4 mM EGTA.

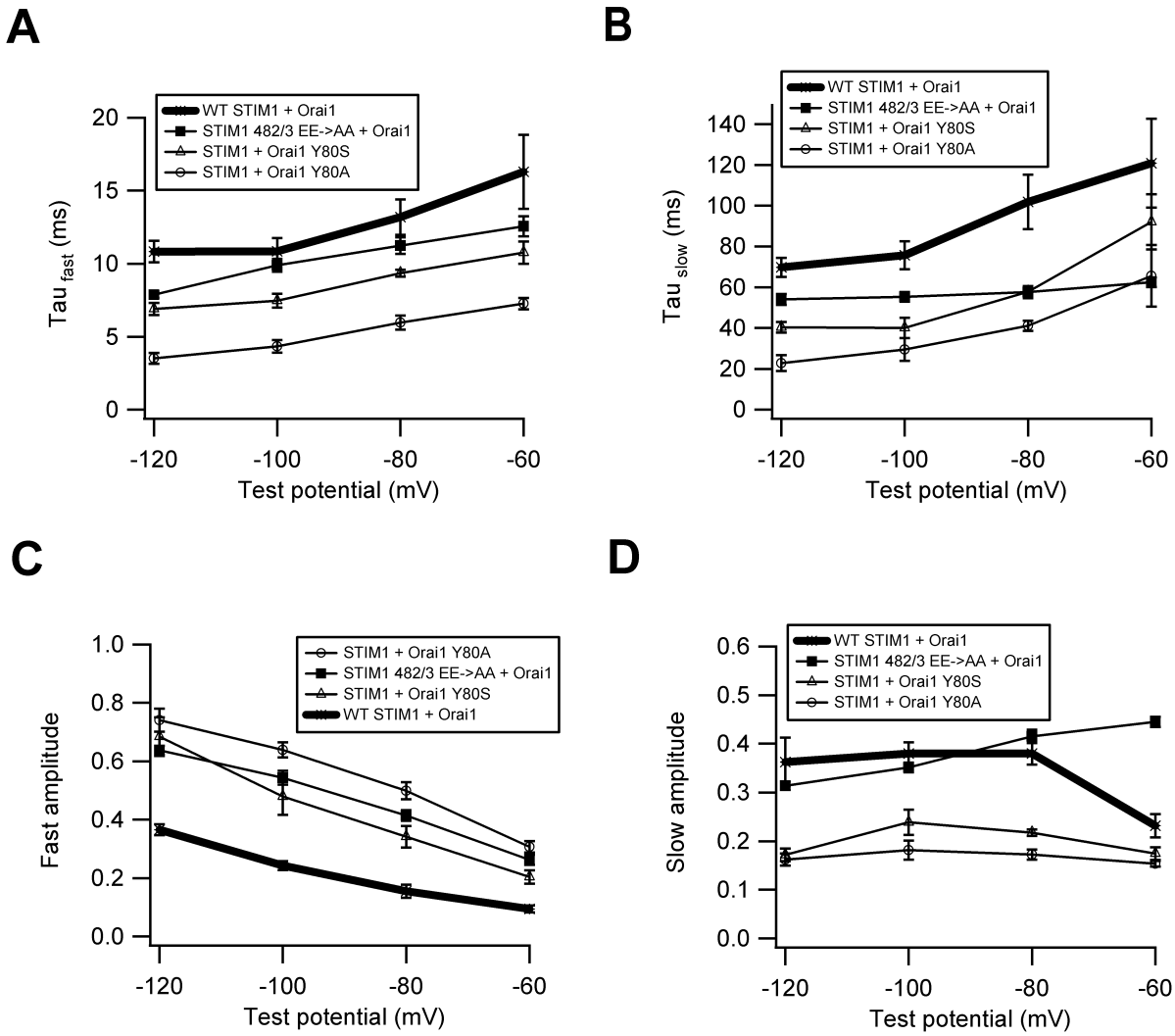

Fig. S8. Acceleration of inactivation kinetics by mutant STIM1 and Orai1 constructs. (*A–D*) The biexponential function $I = I_o + A_{1e}^{-t/\tau 1} + A_2\, e^{-t/\tau 2}$ was fitted to I_{CRAC} evoked by hyperpolarizing pulses in 20 mM $Ca^{2+}{}_o$ (representative records are shown in Figs. 1*A*, 2*E*, and 4 *H* and *I*). Each point represents the mean ± SEM. (*A*) Fast time constants of inactivation plotted against test potential. (*B*) Slow time constants of inactivation plotted against test potential. (*C*) Fast amplitudes of inactivation plotted against test potential. (*D*) Slow amplitudes of inactivation plotted against test potential.

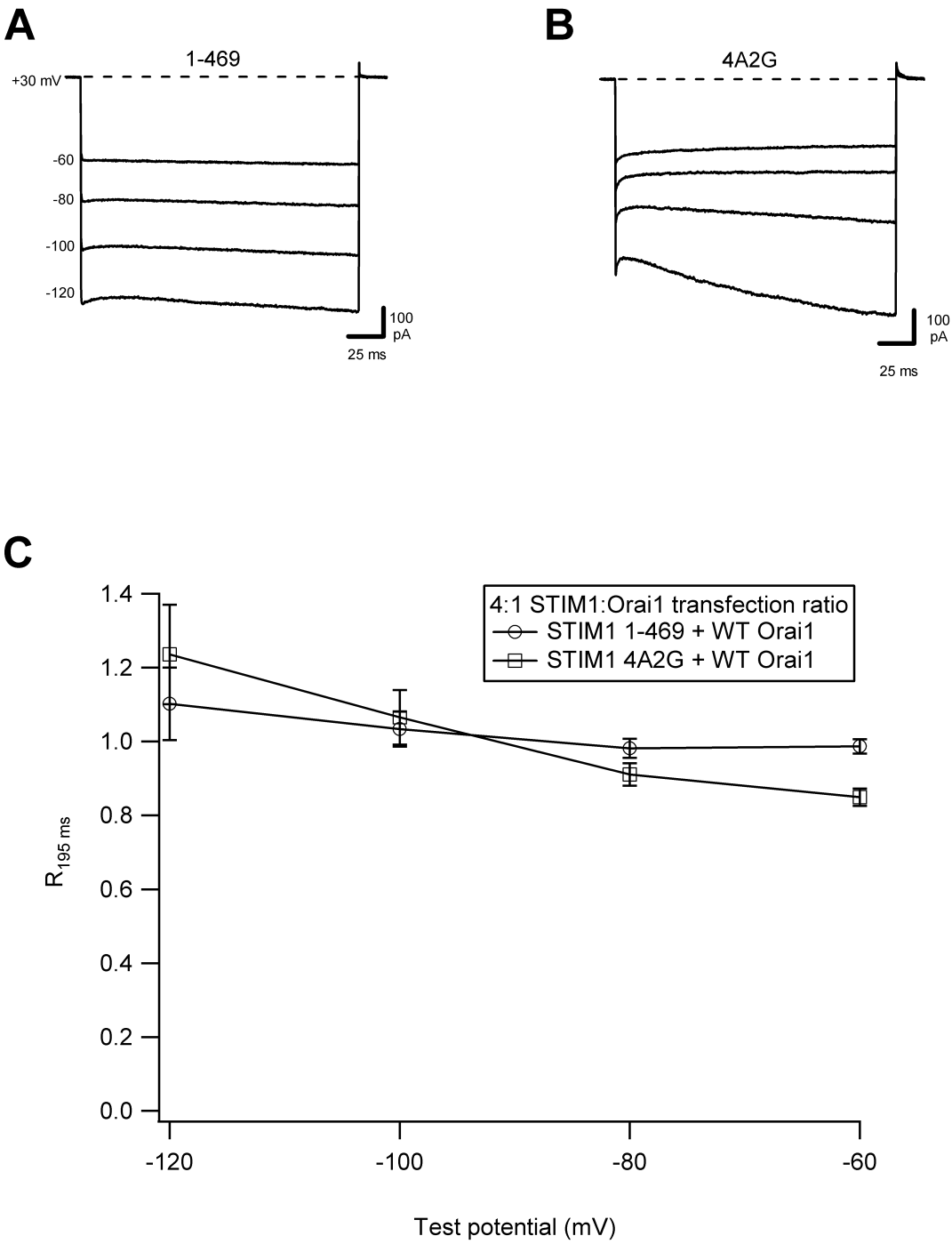

Fig. S9. Absence of inactivation for mutant STIM1 constructs transfected at 4:1 STIM1/Orai1 mass ratio. Currents were elicited in 20 mM Ca^{2+}_o in HEK293 cells cotransfected with the indicated STIM1 construct in 4-fold excess over myc-Orai1. (*A* and *B*) Representative currents during pulses to the indicated voltages for GFP-STIM1$_{1-469}$ (*A*) and myc-STIM1 4A2G (*B*). (*C*) Extent of inactivation, quantified as the residual current remaining at the end of the test pulse ($R_{195\ ms} = I_{195\ ms}/I_{3\ ms}$), plotted against test potential. Each point represents the mean ± SEM of five cells.